Lptv Subspace Analysis of Wind Turbines Data

Laurent Mevel, Ivan Gueguen, Dmitri Tcherniak

LPTV subspace Analysis of wind turbines data

Laurent Mevel[1], Ivan Gueguen[2], Dmitri Tcherniak[3]

[1] *Inria, Rennes, France*
[2] *IFSTTAR, Nantes, France*
[3] *Bruel and Kjaer, SVM, Copenhagen, Denmark*

laurent.mevel@inria.fr

ABSTRACT

The modal analysis of a wind turbine has been generally handled with the assumption that this structure can be accurately modeled as linear time-invariant. Such assumption may be misleading for stability analysis, especially, with the current development of very large wind turbines with complex dynamic behavior (nonlinearity, aeroelastic coupling). Therefore in this paper, the inherent periodically time-varying dynamics of wind turbines (and for rotating systems, in general) is taken into account. Recently a subspace algorithm for modal analysis of rotating systems has been proposed. It is tested on a simulated and real data from a wind turbine.

KEYWORDS : *Modal Analysis, Wind Turbines, Stochastic Subspace Periodic Systems*

INTRODUCTION

The vibration analysis is a primary task for assessing the structural integrity of wind turbines. With the recent development of large and very large offshore wind turbines, this task is becoming increasingly complex and very costly in money and in technical logistics. Developing new techniques that allow an online vibration monitoring and that reduce the need to recurrent inspections and maintenance is, then, one of the most challenging goals of wind engineering for the next years. Vibration monitoring lies on modal analysis. When the wind turbine is assumed to be approximated by a linear time-invariant (LTI) model, this analysis is straightforward and now well known for engineers. Wind turbines are inherently periodically time-varying (LPTV) systems. Under isotropy assumption, these systems can be approximated by a LTI model where the equations of motion are written in the whirling coordinate frame. This transform is called the multi-blade coordinate transform or Coleman transform [1]. Wind turbines are very often subject to important internal (structural properties, asymmetries) and external (gravity load, aerodynamic effects) anisotropies. The periodic dynamics should, then, be taken into account for an accurate characterization. The class of periodic systems is considered to be a bridge between the time-invariant case and the time-varying one. Recently subspace algorithms for LPTV systems have been proposed. These algorithms are applied to both a numerical model of an operating wind turbine and some real data from a Vestas system.

1. FLOQUET THEORY

1.1 Dynamical model

A widely used mathematic representation of dynamical systems is the state space model. For a rotating system, this model writes in continuous-time (See [2]) as follows:

$$\dot{x}(t) = A(t)x(t) + v(t) \tag{1a}$$

$$y(t) = C(t)x(t) + w(t) \tag{1b}$$

where $u(t) \in \mathbb{R}^m$ is the input vector and $y(t) \in \mathbb{R}^r$ the output vector or the observation. The relationship between the input and the output takes place through an intermediate variable which is the state vector $x(t) \in \mathbb{R}^n$. Equation (1a) is named the *state equation* and (1b) is the so-called *output equation* or *observation equation*. The vectors $v(t)$ and $w(t)$ are noises assumed to be white Gaussian. The number n of components in $x(t)$ is the *system order*. Finally, the matrices A, C are respectively named the *dynamic matrix*, the *observation matrix*. The periodicity of the system originates from the periodicity of these matrices, $A(t+T) = A(t)$, $C(t+T) = C(t)$, where the smallest T for which this periodicity is verified is the period of the system. In general, this period is equal to $2\pi/\Omega$ where Ω is the constant rotation speed of the rotor.

1.2 Floquet modal analysis

According to the Floquet theory, if A is continuous in time, or at least piecewise continuous and if an initial condition $x(t_0) = x_0$ is fixed, then a solution of the homogeneous equation $\dot{x}(t) = A(t)x(t)$ is guaranteed to exist (See [3, 4] for further details). The main achievement of the Floquet theory is to show that the solution matrix of $\dot{x}(t) = A(t)x(t)$ can be factorized as a purely periodic matrix $P(t)$ of period T and a time-dependent exponential term function, such that:

$$\Phi(t) = P(t)e^{Rt} \tag{2}$$

Lyapunov has used the result above to transform Equation (1) into an *equivalent autonomous system*, by introducing a new state variable:

$$x(t) = P(t) \cdot z(t) \tag{3}$$

Replacing the state variable x by the new variable z in Equation (1) gives:

$$\dot{z}(t) = Rz(t) + P^{-1}(t)v(t) \tag{4a}$$

$$y(t) = CP(t)z(t) + w(t) \tag{4b}$$

This main result makes the modal analysis straightforward and comprehensive for periodic systems: the modal frequencies are derived from the eigenvalues of R (called *Floquet exponents*) and the modeshapes are the product of the eigenvectors by the periodic matrix $\tilde{C}(t) = CP(t)$. Let $\mu_i = \mu_i^R + i\mu_i^I = \rho_i + i\omega_{p,i}$ be a Floquet exponent. Then, as in time-invariant case the damping ratio and the modal frequency are defined as:

$$\xi_i = \frac{-\rho_i}{|\omega_{p,i}|\sqrt{1 + \rho_i^2/\omega_{p,i}^2}}, \quad f_i = \frac{|\omega_{p,i}|\sqrt{1 + \rho_i^2/\omega_{p,i}^2}}{2\pi} \tag{5}$$

1.3 Stability analysis

The stability or the instability of the system is entirely defined by the characteristic exponents or the damping ratios ξ. In other words, in order to analyze the stability of the periodic system (1), we have just to compute the transition matrix over a period, namely the matrix R. We have thus:

- if all the Floquet exponents have negative real parts (resp., the damping ratios are positive), System (1) is *asymptotically stable* (all the solutions converge to the null solution)
- if there exist a Floquet exponent (resp., a damping ratio) with a positive real part (resp. negative), then System (1) is *unstable* (there is a solution that diverges indefinitely from the null solution)
- if some Floquet exponents (resp. damping ratios) have null real parts (resp. are null) where the other exponents have negative real parts, then the system is in critical state called *the limit of stability* or *neutral stability*. It can be stable or unstable.

1.4 Periodic Subspace Identification

Using the Lyapunov-Floquet transform, the fast discretization of System (1) at a sampling rate τ yields the following periodic system with period $T_d = \frac{T}{\tau}$ (See [5]):

$$z_{k+1} = F z_k + \Gamma_k v_k \tag{6a}$$

$$y_k = \tilde{C}_k z_k + w_k \tag{6b}$$

where $\Gamma_k = \int_0^\tau e^{R\gamma} d\gamma \cdot P_k^{-1}$. The purpose of the identification algorithm below is to extract the discrete Floquet exponents, namely, the eigenvalues of F. From these eigenvalues, one can, then, compute the frequencies and the damping ratios defined in (5).

For periodic systems, one can not mix data arbitrarily. In fact, notions like covariance or correlation have just sense only when they are computed on some subsequences of data (See [6]). For instance, the jth data subsequence is the subsequence of the outputs $(y_{j+iT_d})_i$.

The idea for such systems is to build Hankel matrices with correlations of same subsequences. Consider the Hankel matrix $\mathscr{H}_{p,q}^{(j)}$ defined as:

$$\hat{\mathscr{H}}_{p,q}^{(j)} = \begin{bmatrix} R_1^{(j)} & R_2^{(j)} & \cdots & R_q^{(j)} \\ R_2^{(j+1)} & R_3^{(j+1)} & \cdots & R_{q+1}^{(j+1)} \\ \vdots & \vdots & \vdots & \vdots \\ R_{p+1}^{(j+p)} & R_{p+2}^{(j+p)} & \cdots & R_{q+p}^{(j+p)} \end{bmatrix} \tag{7}$$

where $R_l^{(k)}$ is defined as follows:

$$R_l^{(k)} = \frac{1}{N} \sum_{i=0}^{N-1} y_{k+iT_d} y_{k-l+iT_d} \tag{8}$$

As shown in [7], when N goes to infinity, $R_l^{(k)}$ converge to a function of the correlation of the $(k-l)^{th}$ state subsequence and the $(k-l)^{th}$ data subsequence and of the system matrices. Replacing the $R_l^{(k)}$'s by their expressions, the Hankel matrix writes also:

$$\mathscr{H}_{p,q}^{(j)} = \frac{1}{N} \sum_{i=0}^{N-1} \mathscr{Y}_{j+iT_d}^{+} \mathscr{Y}_{j+iT_d}^{-T} \tag{9}$$

When N goes to infinity, the Hankel matrix $\mathscr{H}_{p,q}^{(j)}$ can be factorized into the observability matrix and the controllability matrix as in the time-invariant case:

$$\mathscr{H}_{p,q}^{(j)} = \mathscr{O}_p^{(j)} \mathscr{C}_q^{(j)} \tag{10}$$

The observability and the controllability matrices are defined this time as in citeMeyer1975:

$$\mathscr{O}_p^{(j)} = \begin{bmatrix} \tilde{C}_j \\ \tilde{C}_{j+1} F \\ \vdots \\ \tilde{C}_{j+p} F^{j+p} \end{bmatrix} \tag{11}$$

$$\mathscr{C}_q^{(j)} = \begin{bmatrix} F G^{(j-1)} & \cdots & F^q G^{(j-q)} \end{bmatrix} \tag{12}$$

where $G^{(k)}$ is the state-output cross correlation of the kth invariant subsequence, when N goes to infinity: $G^{(k)} = \frac{1}{N} \sum_{i=0}^{N-1} z_{k+iT_d} y_{k+iT_d}^T$.

1.5 Algorithm 1

Let build the Hankel Matrix, denoted $\mathscr{H}_{p,q}^{(j+)}$, such that the future data are shifted from the past data by a period T_d:

$$\mathscr{H}_{p,q}^{(j+)} = \frac{1}{N} \sum_{i=0}^{N-1} \mathscr{Y}_{j+(i+1)T_d}^{+} \mathscr{Y}_{j+iT_d}^{-T} \tag{13}$$

Since $\tilde{C}_k$ and $G^{(k)}$ are periodic for all k, we get the following factorization:

$$\mathscr{H}_{p,q}^{(j+)} = \mathscr{O}_p^{(j+T_d)} F^{T_d} \mathscr{C}_q^{(j+T_d)} = \mathscr{O}_p^{(j)} F^{T_d} \mathscr{C}_q^{(j)} \tag{14}$$

Consider the total Hankel matrix that stacks $\mathscr{H}_{p,q}^{(j)}$ and $\mathscr{H}_{p,q}^{(j+)}$:

$$\mathscr{H}_{p,q,tot} = \begin{bmatrix} \mathscr{H}_{p,q}^{(j)} \\ \mathscr{H}_{p,q}^{(j+)} \end{bmatrix} = \begin{bmatrix} \mathscr{O}_p^{(j)} \\ \mathscr{O}_p^{(j)} F^{T_d} \end{bmatrix} \mathscr{C}_q^{(j)} = \mathscr{O}_{p,tot} \mathscr{C}_q^{(j)} \tag{15}$$

An estimate $\tilde{\mathscr{O}}_{p,tot}$ of the total observability matrix $\mathscr{O}_{p,tot}$ can be obtained from a singular value decomposition of the total Hankel matrix (See [7]).

1.6 Algorithm 2

In [8,9], the authors proposed a subspace-based algorithm for the extraction of the Floquet multipliers from the computation of two successive Hankel matrices $\mathscr{H}_{p,q}^{(j)}$ and $\mathscr{H}_{p,q}^{(j+1)}$, then a resolution of a least squares equation. This algorithm estimates the matrix F up to two different time-varying transforms $\hat{T}^{(j)}$ and $\hat{T}^{(j+1)}$, such that the output of the algorithm is related to the desired estimate as $\hat{T}^{(j+1)-1} \hat{F} \hat{T}^{(j)}$. In order to solve this problem some approximation has been made as in [10]. This approximation may hold only for very low rotation speeds. For wind turbines, it makes sense. As a consequence, it will yield to the estimation of the instantaneous transition matrix instead of the Floquet matrix. This matrix is useless for stability analysis but can be useful for damage detection. In this paper, both algorithms will be considered.

2. APPLICATION TO A WIND TURBINE MODEL

This simulation is based on materials from [11]. The Three-blade wind turbine model considered herein is the same as in [12, 13]. This model allows to represent the coupled side-side tower and edgewise blade response of the wind turbine. For the side-side flexibility, we represent it by rendering it into an equivalent spring that connects the hub to the ground. The blades are represented by a rigid body connected to the hub by means of equivalent hinges, whose characteristics in terms of offset from the axis of rotation and stiffness are chosen so as to match the first edgewise natural frequency of the blade. The gravity effect is taken into account. The blade stiffness varies periodically under the effects of its own weight. These effects depend on the blade azimuthal position in its travel round the rotor disk. The mechanical model is sketched in Figure 1. For simplicity, only one blade is represented.

The structural characteristics are reported in Table I. Figure 1 (right) shows the variation of the real part of the system's Floquet exponents against the rotor speed. These parameters go positive for some speed values range; first, between 1.8 rad/s and 3.5 rad/s and second, between 6.8 rad/s and 9.7 rad/s. Since the nominal rotation speed for such large wind turbines is rather close to the first region, the vibration monitoring will focus on the region between 1 and 2 rad/s. Using Matlab, time series data are simulated from the mechanical model. The scenario consists in simulating a rotational speed's acceleration from 1,1 rad/s to 2 rad/s (close to instability) with a step of 0.1rad/s.

Figure 1 : Scheme of the wind turbine model and Campbell diagram - real parts vs. rotor speed

Table 1 : Rotor-tower model system and main parameters

Parameter	Value
Number of blades	3
Rated rotor speed	1.2 rad/s
Hinge offset	25.651
Mass of hub	7.5E+4 kg
Blade mass (movable part)	1.4482E+4 kg
Blade mass (fixed part)	1.0873E+4 kg
Blade static moment	2.7116E+5 kgm
Blade moment of inertia	7.4881E+6 kgm2
Edgewise spring damper	1.7555E+6 Nms
Tower spring stiffness	7.3116E+5 Nm-1
Tower spring damper	1.3294E+4 NSm-1
Edgewise spring stiffness	2.1192E+8 Nm
Rotor radius	75 m

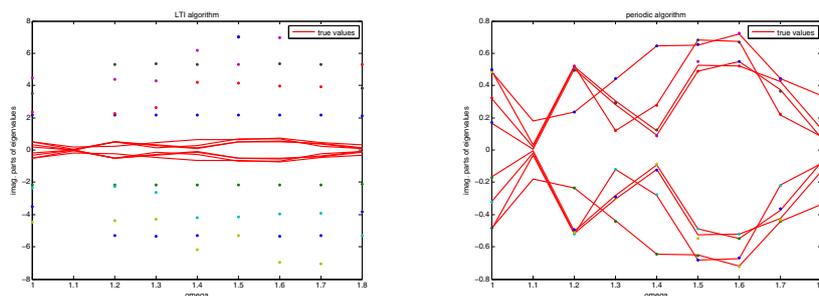Figure 2 : Campbell diagram - real parts vs. rotor speed

Figure 3 : Campbell diagram - imag parts vs. rotor speed

The goal will be to detect the trend to positive values: hence, to detect a change in the values of the Floquet exponents' real parts from their values at the reference. The number of Floquet exponents is equal to the degrees of freedom of the wind turbine: n=4.

It is clear that the Floquet estimated modes match the theoretical values whereas the modes obtained by classical SSI can be very far from the truth (See Figures 2 and 3).

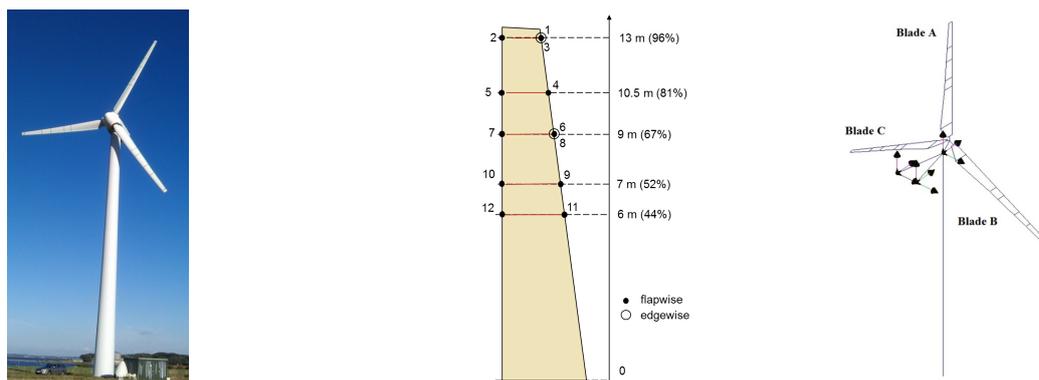## 3. MODAL ANALYSIS OF A IN OPERATIONAL WIND TURBINE

Figure 4 : a) Vestas V27 with blades instrumented with accelerometers; b) Location and orientation of the accelerometers on the blades c) Location of triaxial accelerometers in the nacelle.

We demonstrate the method described above using the data collected from an operating wind turbine during a measurement campaign, which took place from October 2012 until May 2013; the technical details can be found in [14]. A medium size upwind horizontal axis pitch regulated Vestas V27 wind turbine (Figure 4) was used as a test object. Each of the three blades were instrumented by 12 monoaxial accelerometers, 10 in blade's flapwise direction and two in the edgewise direction. In order to catch blade's torsion, the flapwise accelerometers were mounted on both leading and trailing edges of the blades. Thus, five measurement sections along the blade were established; the location of the section was selected using the lowest blade mode shapes generated by FE analysis. In addition, the rotor instrumentation included a pitch sensor and two DC accelerometers; the latter ensured the measurement of the rotor azimuth angle. The data was collected by a 42-channels Bruel and Kjaer LAN-Xi frontend mounted on the rotor hub, and wirelessly transferred to the nacelle. The nacelle instrumentation consisted of three triaxial accelerometers, two located at the rear of the nacelle, and one under the main bearing. In addition, a tachoprobe was used for measuring rotation speed of the high-speed shaft. The rotor and nacelle data streams were synchronized using IRIG-B time stamps extracted from GPS. Simultaneously, the weather parameters were recorded from a nearby weather mast; this included wind speed at different heights, temperature, precipitations and other parameters.

The weather parameters were recorded averaged for every ten minutes intervals. The weather data and the metadata extracted from the measured signals were stored in a database enabling quick search according to different criteria and their combinations. Compared to helicopter rotors, the rotational speed of wind turbine rotors is much lower. The rotor speed of modern wind turbines is regulated by the wind turbine control system and depends on its design. This particular wind turbine was mainly running in two modes: 32 and 43 RPM. For bigger multi-megawatt wind turbines the rotor speed is much lower and might be below 10 RPM. Such low speeds might be problematic for the presented method since it requires information from many rotor revolutions at approximately constant speed, which might be seldom available due to constantly changing wind speed and direction. Using the database, a longest period with almost constant rotor speed was identified: the period spans 8 hours 30 minutes, with the mean wind speed 4.6 m/s, the mean rotor speed 32.2 RPM and almost no pitch activity. During this period, the rotor performed 16417 revolutions. Using the database utility, the continuous time histories spanning the entire period were extracted, decimated down to 102.4Hz sampling frequency and used as an input for the analysis. Additional details regarding the measurement setup can be found in [14, 15].

It has already been shown in [7], that the classical SSI is theoretically wrong when applied to LPTV data. The objective of this experimentation is to qualitatively evaluate if the error is significant when the rotor blade speed is low.
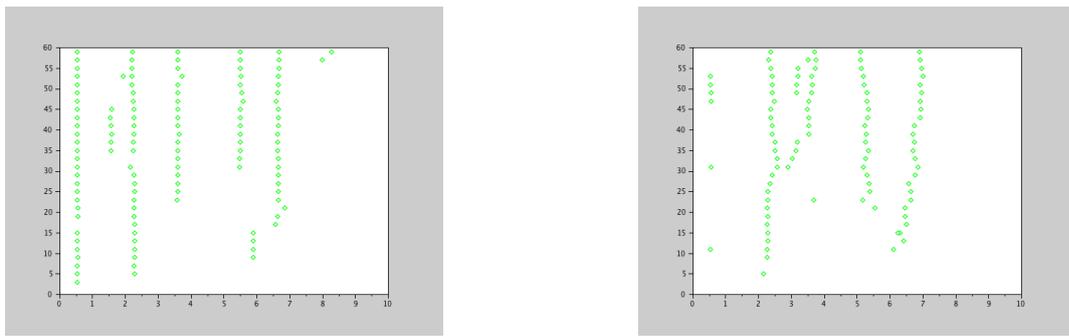

Figure 5 : SSI vs LPTV : short sequence of data

The short sequence data is as such, 12 sensors, a sampling frequency of 200HZ and a rotational frequency of 0.5369Hz for 240000 samples. This is long enough to process a classical SSI but notice that the quality of the LPTV algorithm is related to the number of periods which is very low, around 650. The performance to be expected for the LPTV algorithm on a LPTV system is the same as the classical SSI applied on a LTI system with 650 samples.
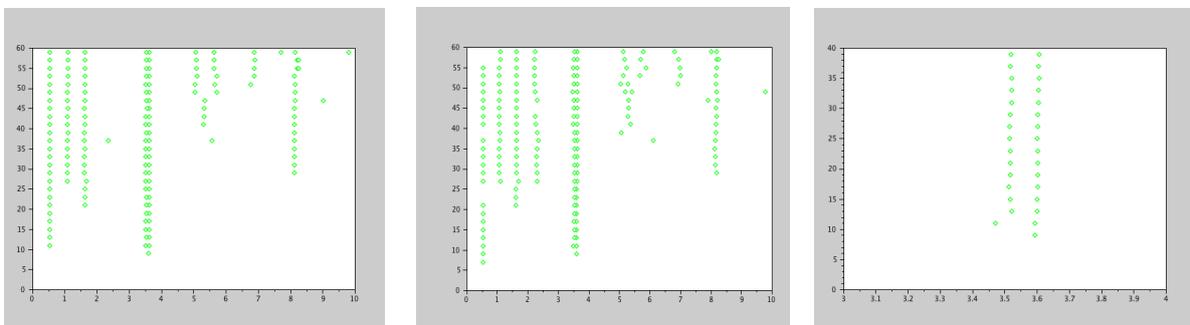

Figure 6 : SSI vs LPTV : long sequence of data

The long sequence is using only six sensors, at 102.4Hz and at a rotating speed of 0.536501Hz. Now, the number of periods for the periodic algorithm is 16K and the algorithm has enough data to

get stable results. As a matter of fact, both the classical and the periodic SSI achieve similar results stressing that the periodic behavior at that speed is not prevalent. Still the periodic SSI is the only one to be guaranteed to be correct. Both algorithms exhibit the correct modes at 3.51HZ and 358Hz as explained in [14, 15].

CONCLUSION

LPTV subspace identification has been investigated for both a simulated and real data from a wind blade systems. Two algorithms were considered. The first one yields Floquet modes of a rotating structure at any given speed. Floquet modes are important because they are symptoms of instability and are thus quantities to monitor in a SHM system. It has been shown that Floquet modes can be significantly different from the modes given by the classical SSI. Another LPTV algorithm is considered. It is shown that at low speed, this algorithm gives similar modes to the classical SSI for that given example. Structural modes can be interesting for assessing damage. There are nonetheless no guarantee that for another example, classical SSI will yield to exploitable results. Still, when the anisotropy of the system is low, a LTI approach can be considered as a rough approximation of the LPTV behavior. Further work will focus on Floquet modes monitoring and computation of uncertainty bounds.

REFERENCES

[1] G. Bir. Multi-blade coordinate transformation and its applications to wind turbine analysis. In *ASME Wind Energy Symposium*, 2008.

[2] G. Genta. *Dynamics of Rotating Systems*. Springer, 2005.

[3] G. Floquet. Sur les équations différentielles linéaires à coefficients périodiques. *Annales scientifiques de l'ENS*, 12:47–88, 1883.

[4] J. J. Dacunha and J. M. Davis. A unified floquet theory for discrete, continuous, and hybrid periodic linear systems. *Journal of Differential Equations*, 251, 2011.

[5] L. Ma and P. A. Iglesias. Quantifying robustness of biomedical network models. *BMC Bioinform*, 3(38), 2002.

[6] R. Meyer and C. Burrus. A unified analysis of multirate and periodically time-varying digital filters. In *Transactions on Circuits and Systems, vol. 22*, 1975.

[7] Ahmed Jhinaoui, Laurent Mevel, and Joseph Morlier. A new ssi algorithm for lptv systems: application to a hinged-bladed helicopter. *Mechanical Systems and Signal Processing*, 42(1):152–166, January 2014.

[8] A. Jhinaoui, L. Mevel, and J. Morlier. Subspace identification for linear periodically time-varying systems. In *Proceedings of the 16th IFAC Symposium on System Identification (SYSID)*, 2012.

[9] A. Jhinaoui, L. Mevel, and J. Morlier. Extension of subspace identification to lptv systems: Application to helicopters. In *Proceedings of the 30th International Modal Analysis Conference (IMAC-XXX)*, 2012.

[10] K. Liu. Identification of linear time-varying systems. *Journal of Sound and Vibration*, 206(4):487–505, 1997.

[11] Ahmed Jhinaoui, Laurent Mevel, and Joseph Morlier. Vibration monitoring of operational wind turbine. In *Proc. 9th International Workshop on Structural Health Monitoring*, Stanford, CA, USA, 2013.

[12] CL Bottasso and S Cacciola. Model-independent periodic stability analysis of wind turbines. *Wind Energy*, 2012.

[13] CL Bottasso and S Cacciola. Periodic stability analysis of wind turbines. *EWEA 2012 Annual Event, Copenhagen, Denmark*, 2012.

[14] Dmitri Tcherniak and GC Larsen. Applications of oma to an operating wind turbine: now including vibration data from the blades. In *5th international operational modal analysis conference (IOMAC), Guimaraes*, 2013.

[15] Shifei Yang, Dmitri Tcherniak, and Mathew Allen. Modal analysis of rotating wind turbine using multiblade coordinate transformation and harmonic power spectrum. In *32th international modal analysis conference (IMAC), Orlando*, 2013.